# Modelling of a Hydro-Pneumatic System for Heave Compensation

John Kenneth Hatletvedt
Department of Engineering Sciences
University of Agder
Grimstad N-4898, Norway
Email: jk_dy@hotmail.com

Kristian Gjerstad
MHWirth AS
New Services and Drilling Systems
Stavanger N-4033, Norway
Email: Kristian.Gjerstad@mhwirth.com

Jing Zhou
Department of Engineering Sciences
University of Agder
Grimstad N-4898, Norway
Email: jing.zhou@uia.no

***Abstract*—This paper presents a mathematical model of the dynamic behaviour of a *passive* heave compensation system. The main purpose is to develop a model that enables cost-efficient prototyping and testing of the control system in an *active* heave compensator. The physics are described by first principles, and result in 21 ordinary differential equations. Temperature calculations are included as an option during simulation in order to investigate its effect on the results. Similarly is a non-ideal gas law (Redlich-Kwong equation) implemented and compared to the ideal gas law. Verification against field data shows that the model is in good accordance with real-life drilling operations. It is further shown that simulation with ideal gas law only gives small deterioration of the results, while neglecting temperature variations has a bigger impact on the dynamics.**

## I. Introduction

In offshore drilling from a floater it is common that the drill string is connected to a heave compensation system that reduces the string motions and the forces on the string/drill bit when the rig itself moves with the sea waves. We consider a semi active crown block mounted heave compensation system (CMC) where the the active control system typically is switched off during drilling, and is switched on when the drill bit is off bottom before the string is put in slips.

In this paper we develop a model of the passive part of the semi active compensation system. A sketch of the system can be seen in Fig. 1, where passive mode is obtained by closing the line to the HPU in the isolation valve. The main purpose of the model is to use it for testing of the active control system in a simulator environment. Such simulator based testing has been found to be both cost and time efficient.

The system is divided into two sections: the hydraulic side (green) and the pneumatic side (blue). The drilling equipment is attached to the travelling block, which is connected to the plunger piston via the crown block. The plunger piston is the main driver of the system. As this piston moves, hydraulic oil will be pushed from the plunger cylinder to the piston accumulator, via hydraulic piping. The accumulator separates the hydraulic side from the pneumatic side by a piston.

As the accumulator piston moves, the gas in the pneumatic system will compress and give flow between the accumulator and an auxiliary volume. The gas compression and dynamics will make the pneumatic system act like a spring-damper system, and thus compensate for the rig heave movement. The force equalizer cylinders in Fig. 1 are connected to the pneumatic system and are designed to reduce load variation over the complete piston stroke.

The authors would like to thank Christian H. Andersen, MHWirth Horten and the University of Agder for valuable inputs and funding of this paper.

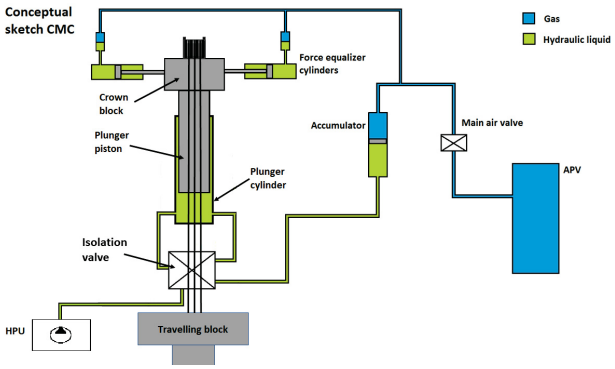


Fig. 1: Conceptual sketch of the compensation system at hand

When developing a model for the purpose of testing a real system, it is important to find the right balance between the level of details/accuracy on one side and simplicity on the other side. In this paper, a transient model based on a set of 21 *ordinary* differential equations is developed. The hydraulic liquid and the gas are lumped together into four control volumes each. The model accounts for dry friction, viscous effects, non-ideal Redlich-Kwong (RK) gas behaviour and temperature variation in the gas system.

## II. Theoretical Background

### A. Equations of State

The equation of state (EOS) gives the relationship between the pressure $p$, the density $\rho$ and the temperature $T$ for a fluid.

*1) Liquid:* For the hydraulic liquid, under isothermal conditions, the EOS can be approximated by the linear relationship [1],

$$\rho = \rho_0 + \frac{\rho_0}{\beta}\left(p - p_0\right), \tag{1}$$

where $\beta$ is the bulk modulus and $\rho_0$ and $p_0$ are nominal density and pressure respectively.

*2) Gas:* When modelling the pneumatic system, there are many EOS' to choose from [2], [3]. In [2] an overview over the most common classes of EOS' can be found. The Redlich-Kwong, Soave-Redlich-Kwong and Peng-Robinson are very often encountered in modelling of gas systems in the oil- and gas industry [4]. Based on comparison of these equations in [4], the RK EOS was found to be applicable for the pneumatic modelling in this paper, as it is assumed that the pneumatic system will not experience any phase changes. The RK EOS is given by [4],

$$p = \frac{RT}{V_m - b} - \frac{a}{\sqrt{T} V_m (V_m + b)}, \tag{2}$$

where,

$$V_m = \tfrac{1}{\rho},\ a = 0.42748 \tfrac{R^2 T_c^{5/2}}{p_c},\ b = 0.08664 \tfrac{RT_c}{p_c},$$

and with $R$ being the specific gas constant. $T_c$ and $p_c$ are the critical temperature and critical pressure, respectively. Note, however, that in some of the simulations the RK EOS is replaced by the ideal gas law ($pV = nRT$) for comparison.

### B. Fluid Dynamics

In this section, some of the governing fluid dynamic equations used in the model is presented or derived. We consider a fluid segment $n$ with volume $V_n$, length $L_n$ and uniform density within $V_n$. The volumetric flow rate and density out of the segment are $q_n$ and $\rho_n$ respectively, as shown in Fig. 2. This is denoted a *lumped* (or averaged) approach. Flow and density into $V_n$ is coming from segment $n-1$ as indicated by the indexes in the figure.

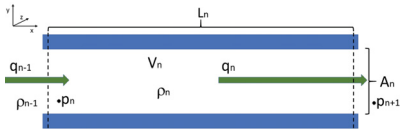


Fig. 2: Conceptual sketch of a fluid volume with flow in and out

*1) Conservation of Mass:* Conservation of mass ($m_n$) for a compressible (generic) fluid can now be formulated as,

$$\dot{m}_n = \frac{d}{dt}(\rho_n V_n) = \rho_{n-1} q_{n-1} - \rho_n q_n. \tag{3}$$

We emphasis that $\rho_n$ is the *average* density of the fluid in $V_n$.

*2) Conservation of Momentum:* We follow the lumped approach from the previous section and also assume that flow is fully developed over the cross-sectional area $A_n$, and that $A_n$ is uniform over the length of the segment. It can then be shown [5] that the derivative of the flow rate can be expressed so that,

$$\dot{q}_n = \frac{A_n^2}{m_n}(\Delta p_{dyn} + \Delta p_f),\ \Delta p_{dyn} = p_n - p_{n+1}, \tag{4}$$

with $\Delta p_f$ being the frictional pressure drop over $V_n$. $\Delta p_f$ is here defined by,

$$\Delta p_f = -f_D \frac{\rho_n L_n v_n^2}{2 D_n},\ v_n = \frac{q_n}{A_n}, \tag{5}$$

where $f_D$ is the Darcy friction factor, $v_n$ is the fluid bulk velocity and $D_n$ is the pipe diameter. If other losses due to bends and valves are present in the system, these can be included by adding them in the same way as $\Delta p_f$.

*3) Conservation of Energy:* To obtain an expression for temperature, consider the first law of thermodynamics,

$$\Delta U = Q - W. \tag{6}$$

Here, $\Delta U$ is the change in internal energy of the system, $Q$ is the heat supplied *to* the system, and $W$ is the work done *by* the system *on* its surroundings. In thermodynamics it is often common to set up the energy balance in terms of enthalpy. Introducing enthalpy as,

$$H = U + pV, \tag{7}$$

and accounting for mass flow, [6] shows that the energy balance can be written on a mass flow basis as,

$$m\frac{dh}{dt} = \dot{m}_{in}(h_{in} - h_{cv}) - \dot{m}_{out}(h_{out} - h_{cv}) + Q - W + V\dot{p}, \tag{8}$$

with $h$ being the specific enthalpy, defined as $\frac{H}{m}$. Note that $W$ will include the boundary work done by the piston.

Considering the RK EOS, its time derivative can be written as,

$$\dot{p} = \frac{\partial p}{\partial T}\frac{dT}{dt} + \frac{\partial p}{\partial V_m}\frac{dV_m}{dt}. \tag{9}$$

As the RK EOS is a non-ideal gas equation, the enthalpy will be a function of both pressure and temperature. To find an expression for the enthalpy, we utilize residual properties as described in [7]. By combining the ideal and residual properties, the enthalpy for a non-ideal gas is obtained. Solving its time derivative and putting the expressions into (8), togehter with (9), the rate of change in temperature can be found from rearranging (8) in terms of temperature,

$$\dot{T} = \frac{H_{in} - H_{out} - h\frac{dm}{dt} + Q - W + \left(V\frac{\partial p}{\partial V_m} - m_{cv}\frac{\partial h}{\partial V_m}\right)\dot{V}_m}{m_{cv}\frac{\partial h}{\partial T} - V\frac{\partial p}{dT}}, \tag{10}$$

with,

$$\begin{aligned}
\dot{V}_m &= \tfrac{-1}{\rho_n^2}\dot{\rho}_n,\\
H_{in}(\dot{m}_{in}(h_{in} - h_{cv}),&\quad H_{out}(\dot{m}_{out}(h_{out} - h_{cv}),\\
\tfrac{\partial p}{\partial V_m} &= -\tfrac{RT}{(V_m - b)^2} + \tfrac{a(2V_m + b)}{\sqrt{T} V_m^2 (V_m + b)^2},\\
\tfrac{\partial p}{\partial T} &= \tfrac{R}{V_m - b} + \tfrac{a}{2T^{\frac{3}{2}} V_m (V_m + b)},\\
\tfrac{\partial h}{\partial V_m} &= -\tfrac{bRT}{(V_m - b)^2} + \tfrac{a\sqrt{T}}{(\sqrt{T} V_m + b)^2} + \tfrac{3a}{2\sqrt{T} V_m (V_m + b)},\\
\tfrac{\partial h}{\partial T} &= c_p + \tfrac{bR}{V_m - b} + \tfrac{aV_m}{2\sqrt{T}(\sqrt{T} V_m + b)^2} + \tfrac{3a}{4T^{\frac{3}{2}} b}\, ln\left[\tfrac{V_m + b}{Vm}\right].
\end{aligned}$$

## III. Hydraulic and Mechanical Modelling

### A. General for Hydraulics

The liquid flow system is divided into four volumes as shown by the numbers $1-4$ in Fig. 3, where also the positive flow direction is shown by arrows.

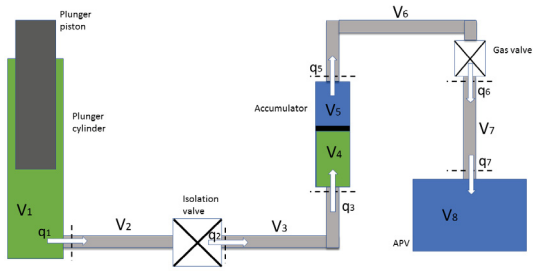


Fig. 3: Simplified drawing of the system with positive flow direction and numbering of segments

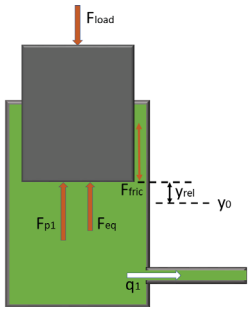


Fig. 4: Sketch of plunger cylinder

For the hydraulic modelling, the energy balance is neglected. Compared to gas, the temperature variation in liquids will be of less importance, and constant temperature is assumed. Also the hydrostatic pressure components are ignored. These can, however, easily be added if the heights of the sensors are known.

For the hydraulic calculations, pressure will appear as a state variable. Simplified conservation of mass for the four liquid volumes is now obtained by combining the EOS for the liquid (1) by the generic conservation of mass (3), and assuming that the density is constant in space [8]. Expressed with the volume index $n$ it is then given by,

$$\dot{p}_n = \frac{\beta}{V_n}\left(q_{n-1} - q_n - \dot{V}_n\right), \; n = 1..4, \tag{11}$$

with $q_0$ being just a dummy variable equal to zero.

### B. Plunger Cylinder Mechanics

The plunger cylinder is a single-acting cylinder with one chamber housing a plunger piston. In this model, two different reference frames are introduced: absolute motion and relative motion. Absolute motion is motion relative to the seabed, while relative motion is motion relative to the cylinder.

To fully describe the cylinder dynamics, three state variables are needed: absolute piston velocity $v_{abs}$, absolute piston position $y_{abs}$ and relative piston position $y_{rel}$. The zero point $y_0$ of the relative motion is chosen to be in the middle of the cylinder and can be seen in Fig. 4. The relative motion is defined as,

$$v_{rel} = v_{abs} - v_{rig}, \tag{12}$$

$$\dot{y}_{rel} = v_{rel}, \tag{13}$$

where subscript *abs* refers to absolute motion, and the subscript *rig* refers to the vertical rig heave motion. Note that $v_{rig}$ is an input signal to the system.

$F_{load}$ is the total force from the load including the hook load and the forces from the piston and the crown block. It is beyond the scope of this paper to investigate these effects in detail. We will here model this force as a constant average force $F_0$ added together with a varying/dynamic force $\Delta F_{dyn}$ that results from the string motion given by $y_{abs}$ and $v_{abs}$. Since we only treat drilling operations where the bit is on bottom, the velocity of the bottom of the string will be given by the rate of penetration (ROP), which is very small and negligible compared to $v_{abs}$. Thus, the dynamic force can be simplified by spring-damper equations, which leads to the following expression for the total load,

$$F_{load} = F_0 + \Delta F_{dyn} = F_0 + k_{eq} \cdot y_{abs} + c_{eq} \cdot v_{abs} \tag{14}$$

where $k_{eq}$ is an equivalent spring coefficient for the entire string and $c_{eq}$ is an equivalent damping factor. Both $F_0$, $k_{eq}$ and $c_{eq}$ are tuned manually so that the model matches log data. Note that this is a very simplified approach, and only used for obtaining load characteristics that are similar to the logged data.

$F_{p1}$ is the hydraulic pressure force acting on the piston, and $F_{eq}$ are the force exerted by the force equalizer cylinders. The latter is obtained from empirical table data. Lastly, $F_{fric}$ is the friction between the piston and the hydraulic oil, and is expressed by,

$$F_{fric} = sign(v_{rel})\; c_{piston}\; v_{rel}, \tag{15}$$

where $c_{piston}$ is the friction coefficient, and is manually tuned.

Putting these expressions into Newtons 2nd law gives the acceleration of the plunger piston as,

$$a_{abs} = \frac{F_{p1} + F_{eq} - F_{fric} - F_{load}}{m_{piston}}, \tag{16}$$

with $m_{piston}$ being the piston mass. From (16) the absolute velocity and position can be found as,

$$\dot{v}_{abs} = a_{abs}, \tag{17}$$

$$\dot{y}_{abs} = v_{abs}. \tag{18}$$

### C. Plunger Cylinder Hydraulics

Conservation of mass is obtained from (11) with $n = 1$ (and $q_0 = 0$), which gives,

$$\dot{p}_1 = \frac{\beta}{V_1}\left(-q_1 - \dot{V}_1\right). \tag{19}$$

The change in volume is dependent on the relative velocity of the piston, and is given by,

$$\dot{V}_1 = A_{piston} \cdot v_{rel}, \tag{20}$$

where $A_{piston}$ is the cross-sectional area of the plunger piston.

A static orifice equation is used to calculate the flow in/out of the cylinder, which is given by [9],

$$q_1 = C_D A_2 \sqrt{\frac{2}{\rho} \Delta p_{dyn}}, \tag{21}$$

where $C_D$ is the discharge coefficient, $A_2$ is the cross sectional area of pipe connected to the outlet, and $\Delta p_{dyn} = p_1 - p_2$.

### D. Hydraulic Piping

The hydraulic pipes have a constant cross-sectional area, and a sketch of the piping is depicted in Fig. 2. For each of the two liquid pipe volumes $V_2$ and $V_3$ (ref. Fig. 3), we have the two state variables $q_n$, and $p_n$, where the subscript $n$ denotes numbering of the volumes. The flow rate going into a volume $V_n$ is the flow out of the former volume, and is therefore known. The dynamic flow rate out of volume 2 and 3 is given by (4) with the addition of the pressure drops over the valve and bends,

$$\dot{q}_n = \frac{A_n^2}{\rho_0 V_n} (\Delta p_{dyn} + \Delta p_{valve} + \Delta p_{bend} + \Delta p_f), n = 2, 3, \tag{22}$$

with $\Delta p_{valve}$ being pressure drop over the valve and $\Delta p_{bend}$ being pressure drop over bends.

Pressure drops due to bends and viscous friction are calculated via the Darcy-Weisbach equation [10] with the sign convention in (5). For laminar flow ($Re < 2500$) the friction factor is given by,

$$f_D = \frac{64}{Re}, \; Re = \frac{D_n v_n \rho_n}{\mu}, \tag{23}$$

where $Re$ is the Reynolds number and $\mu$ is the fluid viscosity. For turbulent flow ($Re > 2500$), the Haaland equation [11] is used to find the friction factor,

$$\frac{1}{\sqrt{f_D}} = -1.8 log_{10} \left[ \left( \frac{\frac{\epsilon}{D}}{3.7} \right)^{\frac{10}{9}} + \frac{6.9}{Re} \right]. \tag{24}$$

Pressure drop over bends are calculated by inserting the bend coefficient $K_b$, which is found in tables, in the Darcy-Weisbach equation,

$$\Delta p_{bend} = -K_b \frac{v_n^2 \rho_n}{2}. \tag{25}$$

Pressure drop over the valves are calculated via the orifice equation,

$$\Delta p_{valve} = -\frac{\rho_0}{2 C_D^2 A_n^2} q_n^2, \; n = 2, 3. \tag{26}$$

As there are no moving parts in the piping, the volume variation in (11) is zero, and the conservation of mass can be written as,

$$\dot{p}_n = \frac{\beta}{V_n} \cdot (q_{n-1} - q_n), \; n = 2, 3. \tag{27}$$

### E. Accumulator (hydraulic side)

The piston accumulator separates the liquid from the gas. The inertial effects from the rig heave is neglected for the accumulator, giving only one frame of reference. Hence, we have two state variables: piston velocity $v_{acc}$ and piston position $y_{acc}$. Hydraulic and pneumatic pressure forces, $F_{p4}$ and $F_{p5}$ respectively, will act on the piston as shown in Fig. 5. Putting this into Newtons 2nd law, and adding the gravitational force from the piston mass $F_{mass}$, and the friction force, $F_{fric}$, gives the acceleration of the accumulator piston as,

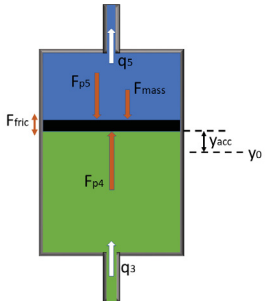


Fig. 5: Sketch of the piston accumuator. Green indicates hydraulic liquid while blue indicates gas

$$a_{acc} = \frac{F_{p_4} - F_{p_5} - F_{mass} - F_{fric}}{m_{acc}}, \tag{28}$$

with $m_{acc}$ being the piston mass. From this expression the piston velocity and position can be found as,

$$\dot{v}_{acc} = a_{acc}, \tag{29}$$

$$\dot{y}_{acc} = v_{acc}. \tag{30}$$

The pressure can be calculated in the same manner as for the plunger cylinder. Thus, from (11) with $n = 4$ we get,

$$\dot{p}_4 = \frac{\beta}{V_4} \left( q_3 - \dot{V}_4 \right). \tag{31}$$

The rate of change of volume for the accumulator is given by,

$$\dot{V}_4 = A_{acc} \cdot v_{acc}, \tag{32}$$

where $A_{acc}$ is the cross-sectional area of the accumulator.

## IV. Pneumatics

### A. General for Pneumatics

The volumes that contain gas are denoted $V_5 - V_8$ in Fig. 3, and positive defined flow direction is *from* the accumulator, *to* the APVs.

Due to the high compressibility of gas compared to liquid, the densities will be modelled explicitly as *state variables*. This is obtained by reorganizing the generic conservation of mass in (3),

$$\dot{\rho}_n = \frac{1}{V_n} \left( \rho_{n-1} q_{n-1} - \rho_n q_n - \rho_n \dot{V}_n \right), \; n = 5...8. \tag{33}$$

The density of a gas is more sensitive to temperature changes than liquids [12]. Therefore, temperature will appear as an additional state variable in the pneumatics. The pressure variables $p_n$ are not state variables, but will be obtained from $\rho_n$ and $V_{m,n}$ by using the static RK EOS (2).

When the gas flows into a volume, perfect mixing is assumed. This means that the temperature, density and pressure

will be uniformly distributed across the volume, and the outflow term $\dot{m}_{out}(h_{out}-h_{cv})$ in the temperature equation will be zero (because $h_{out} = h_{cv}$). For $n = 5...8$ (10) simplifies to,

$$\dot{T}_n = \frac{\dot{m}_{in}(h_{in} - h_{cv}) + Q - W + \left(V\frac{\partial p}{\partial V_m} - m_{cv}\frac{\partial h}{\partial V_m}\right)\dot{V}_m}{m_{cv}\frac{\partial h}{\partial T} - V\frac{\partial p}{dT}}, \tag{34}$$

For simplicity, the index $n$ is omitted on the right side of (34).

The flow to/from the force equalizer cylinders (ref. Fig. 1) will to some extent affect the total system, but it is assumed that this effect will be relatively small compared to the flow between the accumulator and APV's. For simplicity, these are represented by just adding an extra volume to the gas piping.

### B. Accumulator Pneumatics

The total accumulator volume is constant, and the volume on the gas side ($V_5$) will change opposite to the volume on the liquid side ($V_4$). Since the piston motion for the accumulator is already found, and the rate of change of $V_4$ is described in (32), the gas volume is given by $\dot{V}_5 = -\dot{V}_4$.

The rate of change in density can now be obtained by using (33) and recognizing that the flow rate in ($q_4$) is defined to be zero,

$$\dot{\rho}_5 = \frac{1}{V_5}\left(-\rho_5 q_5 - \rho_5\dot{V}_5\right) = \frac{1}{V_5}\left(-\rho_5 q_5 + \rho_5\dot{V}_4\right). \tag{35}$$

There is one pipe connected to the gas side of the accumulator. As for the hydraulic liquid, the gas flow in/out of the accumulator is given by a static orifice equation,

$$q_5 = C_D A_6\sqrt{\frac{2}{\rho_5}\Delta p_{dyn}}. \tag{36}$$

Given the assumptions and observations described in subsection IV-A, the rate of temperature change $\dot{T}_5$ can be found using (34).

### C. Pipe Pneumatics

Similar to the hydraulic pipes, the gas pipes have constant cross-sectional area (ref. Fig. 2). As there are no moving parts in the piping, the rate of change of density can be be obtained from (33) with $\dot{V}_n = 0$. Thus,

$$\dot{\rho}_n = \frac{1}{V_n}(\rho_{n-1}q_{n-1} - \rho_n q_n),\ n = 6, 7. \tag{37}$$

The conservation of momentum in (4) yields for compressible flow in general, and will therefore be applicable for gas flow. With the addition of the losses for bends and valves, and $A_n$ being the cross-sectional area of the gas pipes, the equation can be expressed so that,

$$\dot{q}_n = \frac{A_n^2}{\rho_n V_n.}(-\Delta p_{dyn} + \Delta p_{valve} + \Delta p_{bends} + \Delta p_f), n = 6, 7. \tag{38}$$

The pressure terms in (38) are calculated in the same manner as for the hydraulic pipes. Equation (23) is used for calculation of the laminar friction factor and (24) is used for the turbulent friction factor.

As there are no external work being done in the piping, the work term $W$ in (34) can be set to zero (no moving parts) to obtain $\dot{T}_n$ ($n = 6, 7$).

### D. Air Pressure Vessel Pneumatics

The Air Pressure Vessels (APVs) are divided into two groups: working APVs and standby APVs. The working APVs provide an auxiliary volume for the gas to enter, while the standby APVs provide air volumes at higher pressure making it possible to vary the system pressure. In this paper it is assumed that the working APV volume is constant during operation.

As for the gas side of the accumulator, the derivative of the density is based on (33) with $\dot{V}_8 = 0$. Since positive flow into $V_8$ is given by the flow out of $V_7$ and the flow out ($q_8$) is defined to be zero, the density equation from (33) simplifies to,

$$\dot{\rho}_8 = \frac{1}{V_8}(\rho_7 q_7). \tag{39}$$

To obtain $\dot{T}_8$, the temperature equation (34) can be simplified in the same manner as for the piping in section IV-C (no moving parts).

### E. Model summary

Following is a short summary of the 21 ODEs that define the state variables in the model, and thus make up its dynamic behaviour.

For hydraulic calculations, the 4 pressure variables are given by (19), (27) and (31), while the flow rate in $V_2$ and $V_3$ are given by (22). The *absolute* velocity and position of the piston in the plunger cylinder are given by (17) and (18) respectively, and the *relative* piston position is given in (13). The velocity and position of the piston in the accumulator are described in (29) and (30).

For the pneumatic calculations, the temperature in the 4 gas volumes are described in (34), while the densities are expressed in (35), (37) and (39). The flow rates in $V_6$ and $V_7$ are given by (38).

## V. Results

The model is verified against log data from a floating rig during drilling operation. The vertical heave velocity of the rig is used as an input signal to the simulations. The relative motion of the plunger cylinder is used for calibrating the load forces. Pressure measurements at four of the volumes are compared with the simulations as presented below. There are no temperature measurements available in the log data. All initial values in the simulations are set to match the initial measurements.

There was an offset difference between the four pressure measurement that was not present in the simulations. Since this offset was independent of any motion and flow rate, the authors concluded that this is caused by bias errors in the measurements and/or hydrostatic pressure components that have not been modelled. To better compare the dynamic behaviour, the pressure measurements are therefore shifted vertically so that this offset is removed. After this shift, the

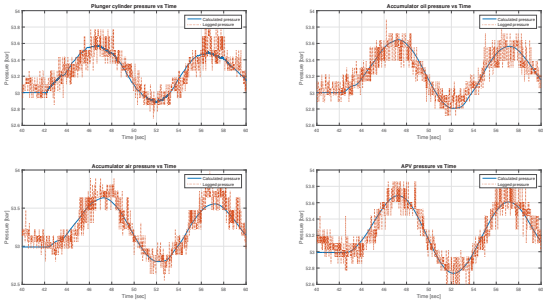


Fig. 6: Logged pressures vs. calculated pressures

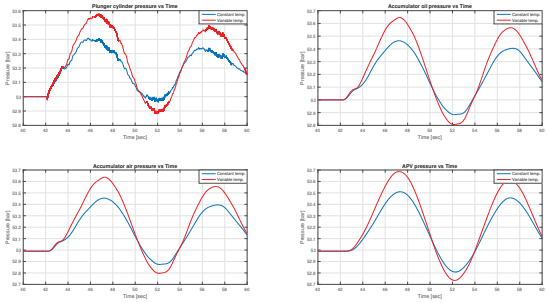


Fig. 7: Pressures with constant temperature vs. variable temperature

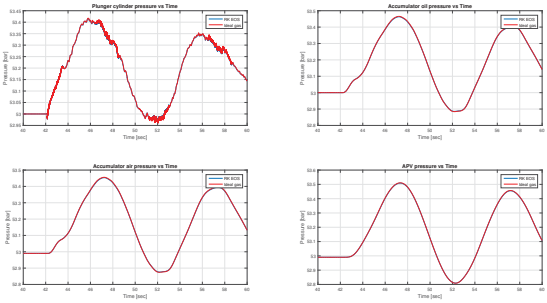


Fig. 8: Ideal pressures vs. Redlich-Kwong pressures

calculated pressure variations vs. logged pressure variations can be seen in Fig. 6. The plots show that the calculations are in good accordance with the data.

To investigate the effects of temperature on the system, a simulation with constant temperature is compared with a simulation with variable temperature. The results are presented in Fig. 7. As can be seen from the plots, if temperature is held constant, the pressure will be lower than for pressures with variable temperature. This is expected, as pressure is increasing with temperature. From examination of the plots in Fig. 7, it is found that the deviation in pressure *variation* from its initial values is in the region 20-40%.

The importance of using non-ideal gas equation is also investigated. For comparison, a simulation with ideal gas at constant temperature is compared to a simulation with the RK EOS at constant temperature. Results can be seen in Fig. 8. The ideal pressures are slightly higher compared to the pressures calculated with the RK EOS. Compared to each other, a difference of about 4% is found.

If comparing this with the general compressibility chart for Nitrogen, this deviation is expected. It is therefore concluded that, the general compressibility chart could be used as an indication of expected deviation between ideal gas and non-ideal gas.

## VI. Conclusions and Further Work

The lumped approach gives good agreement with the log data, and it is shown that the ideal gas equation can be applied with only 4% loss in accuracy for this system. This is in good accordance with the compressibility chart. Depending on desired accuracy of the simulation, this chart can be used as guidance when deciding which EOS to use for future simulations.

It is further shown that neglecting temperature modelling, results in a pressure deviation of 20-40%. It is therefore recommended to include the temperature equations in this type of models.

Further work that could be useful is to include the force equalizers and their corresponding piping in order to investigate the effect on the total system. Also, the model could be divided into more volumes by increasing the number of pipe segments $n$. This would be a straightforward extension of the model/framework presented here. A more comprehensive, but very beneficial, task is to add a drill string and borehole model to obtain more realistic forces from the drill string.

## References


[1] G. Kaasa, O. N. Stamnes, L. Imsland, and O. M. Aamo, "Simplified hydraulics model for estimation of downhole pressure for a managed-perssure-drilling control system," *SPE Drilling & Completion*, no. SPE-143097, pp. 127–138, 2012.

[2] J. O. Valderrama, "The state of the cubic equations of state," *Industrial & engineering chemistry research*, vol. 42, no. 8, pp. 1603–1618, 2003.

[3] D. D. B. M. J. Moran, H. N. Shapiro and M. B. Bailey, *Principles of Engineering Thermodynamics*, 7th ed. Hoboken, NJ: John Wiley & Sons, 2012.

[4] S. Ramdharee, E. Muzenda, and M. Belaid, "A review of the equations of state and their applicability in phase equilibrium modeling." International Conference on Chemical and Environmental Engineering, 2013.

[5] A. K. Gjerstad, "Simplified flow equations for single-phase non-newtonian fluids in couette-poiseuille flow and in pipes - for dynamic modeling of surge and swab pressure in oil well drilling operations," Ph.D. dissertation, UiS, 2014.

[6] S. Skogestad, *Chemical and energy process engineering*. CRC press, 2008.

[7] R. Sandip. (2013) Chemical engineering thermodynamics. [Online]. Available: http://nptel.ac.in/courses/103101004/1

[8] K. Gjerstad, R. W. Time, and K. S. Bjorkevoll, "A medium-order flow model for dynamic pressure surges in tripping operations," *SPE/IADC Drilling Conference and Exhibition, Amsterdam, The Netherlands*, 2013.

[9] M. R. Hansen and T. O. Andersen, *Hydraulic Components and Systems*. University of Agder, 2006.

[10] C. Co., "Flow of fluids through valves, fittings and pipe," New York, N.Y, Tech. Rep., 1982.

[11] S. E. Haaland, "Simple and explicit formulas for the friction factor in turbulent pipe flow," *Journal of Fluids Engineering*, vol. 105, no. 1, pp. 89–90, 1983.

[12] R. Darby and R. P. Chhabra, *Chemical Engineering Fluid Mechanics*, 3rd ed. Boca Raton, FL: CRC Press, 2016.